

## SURFACE PASSIVATION USING DIELECTRIC FILMS: HOW MUCH CHARGE IS ENOUGH?

K.J.Weber, H. Jin, C. Zhang, N. Nursam, W.E. Jellett and K.R. McIntosh  
Centre for Sustainable Energy Systems

College of Engineering and Computer Science  
The Australian National University, Canberra, ACT, Australia 0200  
Email: [klaus.weber@anu.edu.au](mailto:klaus.weber@anu.edu.au), Web: <http://solar.anu.edu.au/>

**ABSTRACT:** It is well known that the recombination of excess carriers at semiconductor surfaces can be substantially reduced by electrostatic charge. The ability to incorporate large charge densities in dielectric films, and to vary the charge density through adjustment of deposition parameters or post deposition treatments, raises an important practical question: how much charge is enough for optimum passivation? We attempt to answer this question through direct measurement of the emitter saturation current density  $J_{oe}$  as a function of applied voltage on samples with a symmetric metal-insulator-semiconductor (MIS) structure. Our results indicate that the impact of applied charge density on surface recombination tends to saturate at charge densities of around  $8 \times 10^{-7} \text{C/cm}^2$  ( $5 \times 10^{12}$  charges  $\text{cm}^{-2}$ ), so that higher charge densities do not offer any increased benefit for surface passivation. While our results are currently confined chiefly to oxide passivated samples, we expect that a similar behavior will be observed for samples passivated with other dielectric films.

**Keywords:** Surface passivation, charge

### 1 INTRODUCTION

Surface passivation has become a critical issue for silicon solar cells, since further improvements in conversion efficiency will be difficult to achieve without improved surface passivation schemes. The importance of surface passivation becomes even greater as the substrate thickness for silicon solar cells is reduced in order to reduce material cost.

Several dielectric materials that are currently of interest for silicon solar cells – such as silicon nitride ( $\text{SiN}_x$ ) and aluminium oxide ( $\text{Al}_2\text{O}_3$ ) – can achieve excellent surface passivation in large part as a result of the presence of a large density of built-in charges. In dielectrics which lack a high charge density in the bulk of the film, the subsequent application of surface charge – by corona charging, for example – has also been observed to dramatically alter the observed surface recombination.

The chief effect of charge is to alter the concentration of majority and minority carriers at the surface. Low rates of surface recombination require low concentrations of one type of carrier – either electrons or holes. Thus, surface recombination can be minimized through the application of either a high density of negative charge (resulting in a low surface electron concentration) or positive charge (resulting in a low hole concentration). For heavily doped or diffused surfaces, a very large charge density would be required to invert the surface, while only a small charge density is needed for accumulation. For this reason, PECVD  $\text{SiN}_x$ , which contains positive charge, can easily be used to passivate heavily doped, n type emitters, while ALD deposited  $\text{Al}_2\text{O}_3$  films with a high negative charge density are particularly useful for the passivation of p type emitters.

The ability to incorporate large charge densities in dielectric films, and to vary the charge density through adjustment of deposition parameters or post deposition treatments, raises an important practical question: how much charge is enough? To date, there is no clear experimental evidence which shows either that surface passivation continues to improve with higher charge densities, or that higher charge densities do not result in

further improvements in surface passivation beyond a critical value of charge density.

In this paper, we attempt to answer this question through direct measurement of the emitter saturation current density  $J_{oe}$  on various test samples. Charging was primarily carried out using a symmetric metal-insulator-semiconductor (MIS) structure described elsewhere [1]. For comparison, on some samples charging was carried out using a corona discharge chamber, either with or without a gate [2].

### 2 EXPERIMENTAL

Samples used for the experiments were FZ (100) and (111) wafers with a dopant concentration of less than  $10^{14} \text{cm}^{-3}$ . Wafers were etched in hydrofluoric/nitric acid solution to remove at least 10µm from each surface, cleaved into quarters and then given a standard RCA clean. Some wafers received a boron diffusion from a liquid  $\text{BBr}_3$  source, other wafers received a P diffusion from a liquid  $\text{POCl}_3$  source while some wafers did not receive a diffusion. A 50-100nm thick thermal oxide was grown at 1000°C followed by a  $\text{N}_2$  anneal at the same temperature for 30 minutes, and a forming gas anneal for 30 minutes at 400°C. This was followed on some wafers by the deposition of 50nm of silicon nitride by low pressure chemical vapor deposition.

For the creation of a symmetric MIS structure, aluminium was evaporated over a circular area onto both sides of each quarter to a thickness of ~5nm. The diameter of the metallised area was at least 5mm larger than the sensing area of the inductive coil for lifetime measurements in order to minimise edge effects. Contact to the Al layers was made using conductive silver paste, while contact to the silicon bulk was made by removing a small amount of oxide in one of the corners of the sample and applying silver paste. The wafer quarter was positioned so that the metallised region was centered over the inductive coil. The metal thickness was carefully

chosen to ensure minimal interference with the lifetime measurement.

For samples that were charged using a corona discharge chamber, a Kelvin probe was used to determine the change in surface potential and hence the charge density. The charge uniformity from these measurements was typically better than 20%.

Lifetime and dark saturation current density ( $J_{oe}$ ) measurements were carried out using the inductively coupled photoconductivity decay technique [3]. Direct measurement of  $J_{oe}$ , rather than the effective surface recombination velocity, has the advantage that it allows the unambiguous separation of surface and bulk recombination. Both lifetime and  $J_{oe}$  were measured at an injection level of  $4 \times 10^{15} \text{cm}^{-3}$ .

For each MIS sample, lifetime and  $J_{oe}$  measurements were carried out while the applied voltage was swept. In the case of undiffused samples, both positive and negative biases were applied while for diffused samples, the bias applied was such as to only result in accumulation conditions. The applied voltage is then easily converted into a charge density.

### 3 MODELED EFFECT OF CHARGE

Fig. 1 shows an example of the effect of charge on the profile of majority carriers, for the case of a lightly doped, p type wafer (background doping  $10^{14} \text{cm}^{-3}$ ) with a surface charge density of  $-4 \times 10^{12} \text{cm}^{-2}$ . Particularly noteworthy is the fact that the electric charge results in an extremely sharp spike in the carrier concentration profile just at the surface, completely unlike the profile obtained from a diffusion.

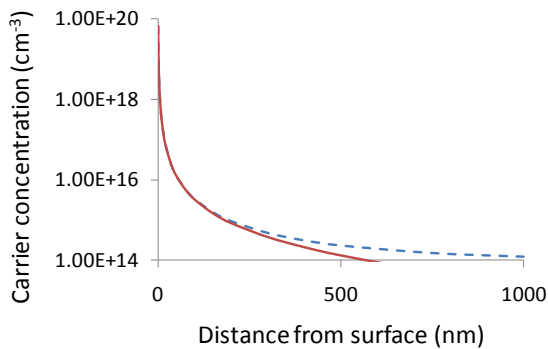


**Figure 1:** Effect of charge on the profile of majority carriers, for the case of a lightly doped, p type wafer (background doping  $10^{14} \text{cm}^{-3}$ ) with a surface charge density of  $-4 \times 10^{12} \text{cm}^{-2}$ . Red solid line: excess hole density; blue dashed line: total hole density

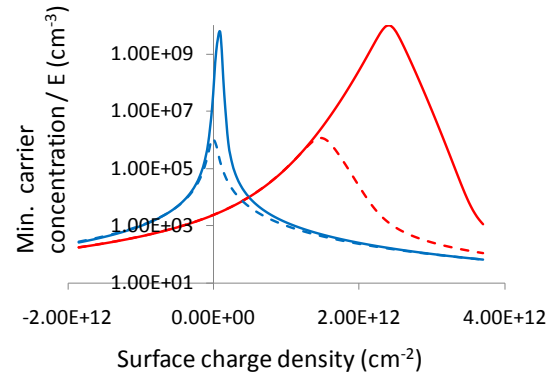
One practical implication is that a surface with a sufficiently high charge density but without a diffusion is extremely effective at minimizing current loss due to the recombination of photogenerated carriers at the front surface, because practically all photogenerated carriers are created in the lowly doped device region and are repelled from the front surface by the presence of a strong electric field. Thus, if a diffusion is not required for current collection (as is the case for a back contact cell) then the best surface passivation is actually offered by an undiffused, charged front surface.

Fig.2 shows the modeled effect of surface charge on the surface minority carrier concentration both in the dark

(equilibrium) and under illumination (or bias), creating a separation of the quasi Fermi levels and therefore a voltage within the device. The illuminated curves have been normalised by dividing the actual surface minority carrier concentration by  $E$ , where  $E$  is defined as

$$E = p \cdot n / p_0 \cdot n_0 \quad (1)$$

where  $p$  and  $n$  are the (bulk) electron and hole concentrations under illumination, and  $p_0$  and  $n_0$  are the corresponding quantities in equilibrium.



**Figure 2:** Modeled effect of surface charge density on surface minority carrier concentration in equilibrium (solid line) and under illumination/bias (dashed line). The curves are for a lightly ( $10^{14} \text{cm}^{-3}$ , blue) and heavily ( $10^{18} \text{cm}^{-3}$ , red) doped p type surface. Modeling was done using the modified Girish model [4].

As has been noted before, at high charge densities, the surface minority carrier concentration becomes independent of substrate doping, particularly in accumulation. It is also interesting to note from fig. 2 that, with an increase in the pn product (corresponding to a higher voltage) there is a shift the position of the peak (usually corresponding to the region of maximum recombination) towards the origin. This shift is hardly noticeable for the lowly doped sample but is quite pronounced for the heavily doped sample. However, in accumulation and strong inversion, the curves for illuminated and unilluminated samples overlap, indicating that the excess minority carrier surface concentration  $n_s$  is related to equilibrium concentration  $n_{0s}$  and the voltage  $V$  by the simple relationship

$$n_s \approx n_{0s} \exp(V/V_T) \quad (2)$$

where  $V_T$  is the thermal voltage ( $\sim 26 \text{mV}$  at room temperature) and the relationship is valid for  $V \gg V_T$ . In this regime, it is possible to easily extract the emitter saturation current density  $J_{oe}$  as a parameter to characterize surface recombination, provided that the wafer bulk is in high level injection.

The surface recombination rate is rate is related to the surface minority carrier concentration by

$$U_S = S n_s \quad (3)$$

where  $S$  is the surface recombination velocity.  $S$  is given by the Shockley-Read-Hall equation and depends on the properties (distribution across the bandgap and capture cross sections) of the interface defects. While  $S$  in

general will vary with varying surface carrier concentrations (in particular,  $S$  will be expected to increase slightly with increasing surface majority carrier concentration), for sufficiently high surface majority carrier concentrations, this dependence is expected to be relatively weak, and one may expect that  $U_s$  will be mainly dependent on  $n$ . This in turn would imply that  $J_{oe}$  is mainly dependent on  $n_0$ . Hence one might expect that, as more and more charge is applied to a surface,  $n_0$  and  $J_{oe}$  will both continue to decrease. Unfortunately, the experimental results show that this is not the case.

#### 4 MEASUREMENT RESULTS

Fig. 3 shows  $J_{oe}$  as a function of applied charge density for three different undiffused samples, while fig. 4 shows results for several different diffused samples. In all cases, we observe saturation of  $J_{oe}$  for sufficiently high charge density. Further, while there is considerable variation from sample to sample,  $J_{oe}$  generally tends to saturate at a charge density of  $5 \times 10^{12} \text{ cm}^{-2}$  or less.

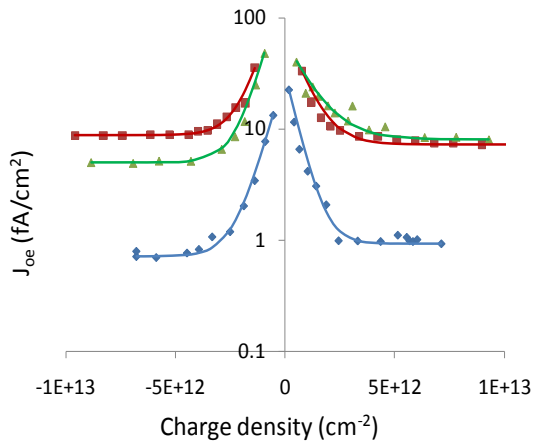


**Figure 3:**  $J_{oe}$  vs charge density for undiffused samples, measured with MIS structure ■ (111), 100nm  $\text{SiO}_2$ , ▲ (100), 50nm  $\text{SiO}_2$  / 50nm LPCVD  $\text{Si}_3\text{N}_4$ , ◆ (100) 50nm  $\text{SiO}_2$ . The lines are fits to the experimental data.

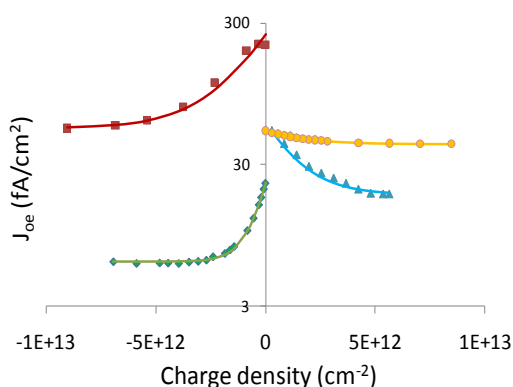


**Figure 4:**  $J_{oe}$  vs charge density for diffused samples: ◆ B, 200  $\Omega/\text{sq}$  (100), 100nm  $\text{SiO}_2$ ; ■ B 200  $\Omega/\text{sq}$  (111) 50nm  $\text{SiO}_2$  / 50nm LPCVD  $\text{Si}_3\text{N}_4$ ; ▲ P diffused, 400  $\Omega/\text{sq}$  (100) 50nm  $\text{SiO}_2$  / 50nm LPCVD  $\text{Si}_3\text{N}_4$ ; ● P diffused, 160  $\Omega/\text{sq}$  (100) 50nm  $\text{SiO}_2$

In principle, a saturation of  $J_{oe}$  with increasing charge

density could be due several reasons.  $J_{oe}$  consists of two components, namely 1) recombination in the emitter (heavily doped bulk) region ( $J_{oe,B}$ ) and 2) recombination at the actual surface ( $J_{oe,S}$ ). For heavy diffusions in particular, the former can often dominate, so that decreases in  $J_{oe,S}$  may not be measurable. In addition, for very low  $J_{oe}$  values, an observed saturation could be due to the limited sensitivity of the measurement equipment.

For most of our experimental data, both of the above possible causes of  $J_{oe}$  saturation can be ruled out. In the undiffused samples,  $J_{oe,B}$  is negligible due to the extremely narrow carrier concentration peak created by charge. Further, the measured saturated  $J_{oe}$  values span a large range, including values that are well above the sensitivity limit of the measurement technique. For the diffused samples, we have estimated the likely contributions from the emitter regions and established upper limits for these contributions in several cases (for example, by attributing the entire measured  $J_{oe}$  to  $J_{oe,B}$  for samples with (100) surfaces, and then measuring (111) samples with the same diffusion profile [5]). Thus, the results can only be explained by a saturation of  $J_{oe,S}$  with increasing charge density.

One source of error in these measurements is introduced by leakage currents through the insulator. Such leakage currents, if sufficiently large, can result in a potential drop across the sample and will be expected to cause a ‘smearing out’ of the observed curves. In this case, the value of the charge density at which  $J_{oe}$  saturation occurs will be overestimated. The leakage current densities for the sample measurements reported here were relatively low, but may still have had some effect on the curves particularly for the diffused samples, which tend to display larger leakage currents.

Fig. 5 shows a comparison of the charge density- $J_{oe}$  trends obtained with different charging techniques. The corona charging technique does not suffer from the potential problem of leakage currents that are an issue with MIS structures. However, it is not always easy to obtain a very uniform charge distribution over the sample, particularly in the absence of a metal grid, which allows the deposited charge to be varied in a more controllable and uniform way. The measurements were carried out on different oxidized, undiffused (100) samples. While the absolute  $J_{oe}$  values vary substantially between the different samples (probably due to differences in the detailed processing conditions) they all a very similar trend in terms of the reduction of  $J_{oe}$  with increasing charge. Importantly, all samples indicate a saturation of  $J_{oe}$  at a charge density of  $5 \times 10^{12} \text{ cm}^{-2}$ .

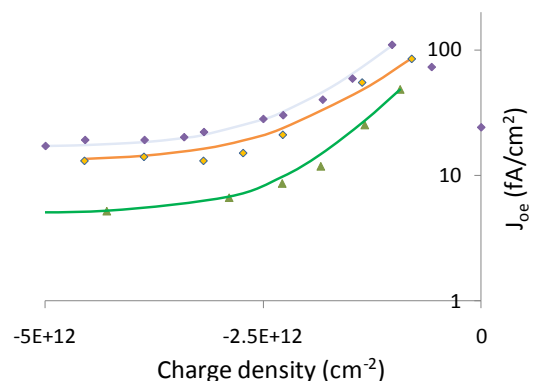


**Figure 5:**  $J_{oe}$  vs charge density for oxidised, undiffused (100) samples charged with different techniques: ◆

corona (with grid) ◆ corona (without grid) ▲ MIS structure. Measurements were done on different samples.

Fig. 6 shows a comparison of experimental results with expected  $J_{oe}$  trends. The expected trends were calculated either by neglecting bandgap narrowing, or with a simplified bandgap narrowing (BGN) model, using the BGN parameters of King et al [6]. The  $J_{oe}$  curves were obtained by calculating the variation in  $n_s$  with applied charge density, and assuming that  $J_{oe}$  is proportional to the surface minority carrier concentration. This calculation neglects the detailed relationship of  $J_{oe}$  to  $n_s$  via the Shockley-Read-Hall equation, but it provides a good first order approximation.

The comparison shows that calculated variation in  $n_s$  does not fit the observed trend well, even when bandgap narrowing is taken into account. The BGN model used neglects degeneracy and will overestimate the pn product at high majority carrier concentrations [7]. Thus, a more accurate BGN model using Fermi-Dirac statistics would be expected to result in a more rapid (predicted) decrease in  $J_{oe}$  with increasing charge density than the BGN model used, and even worse agreement with experimental data. One reason for the observed discrepancy may be the difference between the actual carrier profiles in the near surface region, and the profiles calculated using the classical equation, which neglect quantum mechanical effects [8] and overestimate  $n_s$ . It is possible that a more detailed model taking into account this and other quantum mechanical effects will result in better qualitative agreement.

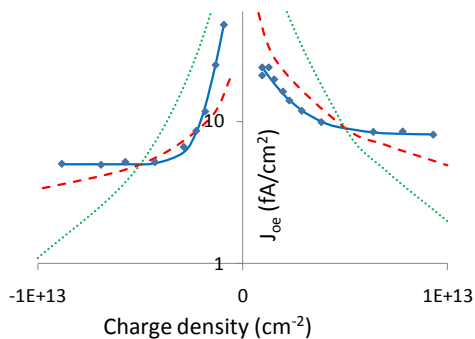


**Figure 6:** Comparison of observed dependence of  $J_{oe}$  on charge density with models. Blue solid line: experimental data; green dotted line: expected dependence assuming no bandgap narrowing; red dashed line: expected dependence taking into account bandgap narrowing.

## 5 CONCLUSIONS

Our experimental results indicate that electrostatic charge can result in a reduction of surface recombination up to a charge density of about  $5 \times 10^{12} \text{ cm}^{-2}$ . However, higher charge densities do not result in a further improvement in surface passivation. While our results are currently confined chiefly to oxide passivated samples, we expect that a similar behavior will be observed for samples passivated with other dielectric films. This is because the reason for the saturation is likely to be related to the concentration profile of carriers in the near-surface region, which is independent of the dielectric film used.

## ACKNOWLEDGEMENTS

The authors would like to thank J. Benick and S. Glunz at the Fraunhofer Institute for Solar Energy Systems for use of their corona discharge system. Financial support for this work from the Australian Research Council is gratefully acknowledged.

## REFERENCES

- [1] W.E. Jellett and K.J. Weber, *Appl. Phys. Lett.* **90**, 042104 (2007)
- [2] S.W. Glunz et al., *J. Appl. Phys.* **86**, 683 (1999)
- [3] D.E. Kane and R.M. Swanson, *Proc. Eighteenth IEEE Photovoltaic Specialists Conference*, 578 (1981)
- [4] A.G. Aberle, S.W. Glunz and W. Warta, *J. Appl. Phys.* **71**, 4422 (1992)
- [5] W.E. Jellett et al., *Proc. 33rd IEEE Photovoltaic Specialist Conference*, 505 (2008)
- [6] R.R. King and R.M. Swanson, *IEEE Transactions on Electron Devices* **38**, 1399 (1991)
- [7] P.A. Altermatt et al., *J. Appl. Phys.* **92**, 3187 (2002)
- [8] Y. Taur et al., *Proceedings of the IEEE*, **85**, 486 (1997)